AD-A154 160 MEMORY EFFECTS IN DYNAMICAL MANY-BODY SYSTEMS: THE ISOMNESIC (CONSTANT-ME..(U) ROCHESTER UNIV NY DEPT OF CHEMISTRY A C BERI ET AL. APR 85 UROCHESTER/DC/85/TR-64 N00014-80-C-0472 F/G 12/1 NL

1/1

UNCLASSIFIED

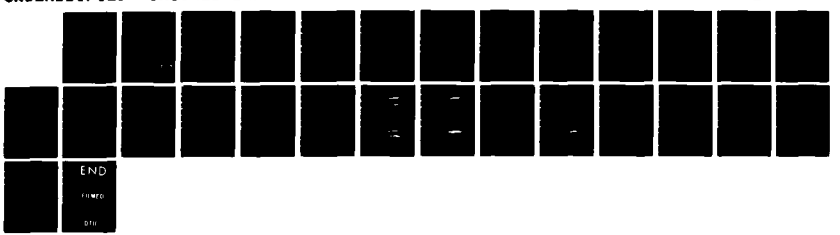

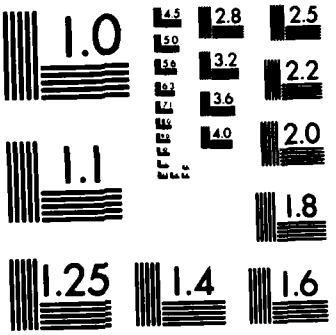

(2)

OFFICE OF NAVAL RESEARCH

Contract N00014-80-C-0472

Task No. NR 056-749

TECHNICAL REPORT No. 64

Memory Effects in Dynamical Many-Body Systems: The Isomnesic (Constant-Memory) Approximation

by

A. C. Beri and Thomas F. George

Prepared for publication

in

Zeitschrift für Physik B: Condensed Matter

Department of Chemistry
University of Rochester
Rochester, New York 14627

April 1985

UNCLASSIFIED

SECURITY CLASSIFICATION OF THIS PAGE

REPORT DOCUMENTATION PAGE

1a. REPORT SECURITY CLASSIFICATION Unclassified	1b. RESTRICTIVE MARKINGS
2a. SECURITY CLASSIFICATION AUTHORITY	3. DISTRIBUTION/AVAILABILITY OF REPORT Approved for public release; distribution unlimited
2b. DECLASSIFICATION/DOWNGRADING SCHEDULE	
4. PERFORMING ORGANIZATION REPORT NUMBER(S) UROCHESTER/DC/85/TR-64	5. MONITORING ORGANIZATION REPORT NUMBER(S)
6a. NAME OF PERFORMING ORGANIZATION Department of Chemistry University of Rochester 6b. OFFICE SYMBOL (If applicable)	7a. NAME OF MONITORING ORGANIZATION Office of Naval Research (Code 413)
6c. ADDRESS (City, State and ZIP Code) River Station Rochester, New York 14627	7b. ADDRESS (City, State and ZIP Code) Chemistry Program 800 N. Quincy Street Arlington, Virginia 22217
8a. NAME OF FUNDING/SPONSORING ORGANIZATION Office of Naval Research 8b. OFFICE SYMBOL (If applicable)	9. PROCUREMENT INSTRUMENT IDENTIFICATION NUMBER Contract N00014-80-C-0472
8c. ADDRESS (City, State and ZIP Code) Chemistry Program 800 N. Quincy Street Arlington, Virginia 22217	10. SOURCE OF FUNDING NOS. PROGRAM ELEMENT NO. 61153N; PROJECT NO. 013-08; TASK NO. NR 056-749; WORK UNIT NO.
11. TITLE Memory Effects in Dynamical Many-Body Systems: The Isomnesic (Constant-Memory) Approximation	
12. PERSONAL AUTHOR(S) A. C. Beri and Thomas F. George	
13a. TYPE OF REPORT Interim Technical 13b. TIME COVERED FROM _____ TO _____	14. DATE OF REPORT (Yr., Mo., Day) April 1985 15. PAGE COUNT 21
16. SUPPLEMENTARY NOTATION Prepared for publication in Zeitschrift für Physik B: Condensed Matter	
17. COSATI CODES FIELD / GROUP / SUB. GR.	18. SUBJECT TERMS (Continue on reverse if necessary and identify by block number) MANY-BODY SYSTEMS, GENERALIZED MASTER EQUATION, MEMORY EFFECTS, (continued on reverse side)

19. ABSTRACT (Continue on reverse if necessary and identify by block number)

Exact numerical solutions of a generalized master equation for a system involving a temporally localizable memory kernel and a constant one are presented. Comparison with an isomnesic (constant-memory) approximation, with the memory kernel reduced to the sum of a local and a constant term, gives excellent agreement. A Markovian version of the problem is also described and found to be inherently ambiguous, devoid of significant physical features seen in the transient regions, but leading to the same steady-state as the isomnesic approximation.

20. DISTRIBUTION/AVAILABILITY OF ABSTRACT UNCLASSIFIED/UNLIMITED ☒ SAME AS RPT. ☒ DTIC USERS ☐	21. ABSTRACT SECURITY CLASSIFICATION Unclassified
22a. NAME OF RESPONSIBLE INDIVIDUAL Dr. David L. Nelson	22b. TELEPHONE NUMBER (Include Area Code) (202) 696-4410 22c. OFFICE SYMBOL

DD FORM 1473, 83 APR EDITION OF 1 JAN 73 IS OBSOLETE.

UNCLASSIFIED

SECURITY CLASSIFICATION OF THIS PAGE

18. ,ISOMNESIC APPROXIMATION,
AGREEMENT WITH EXACT RESULTS,
IMPROVEMENT ON MARKOVIAN APPROXIMATION.

Zeitschrift für Physik B, in press

Memory Effects in Dynamical Many-Body Systems: The Isomnesic (Constant-Memory) Approximation

A. C. Beri and Thomas F. George
Department of Chemistry
University of Rochester
Rochester, New York 14627

Abstract

Exact numerical solutions of a generalized master equation for a system involving a temporally localizable memory kernel and a constant one are presented. Comparison with an isomnesic (constant-memory) approximation, with the memory kernel reduced to the sum of a local and a constant term, gives excellent agreement. A Markovian version of the problem is also described and found to be inherently ambiguous, devoid of significant physical features seen in the transient regions, but leading to the same steady-state as the isomnesic approximation.

I. Introduction

The dynamics of a system of many interacting particles is often treated by partitioning the system into two or more subsystems, one of which, $\mathcal{S}$, comprises the degree(s) of freedom of primary interest, while the others, $\mathcal{R}_1, \mathcal{R}_2, \ldots$, are reservoirs to which $\mathcal{S}$ is coupled.[1] No observations are made on the reservoirs, and the corresponding degrees of freedom are projected out of the equations of motion. A quantum mechanical generalized master equation (GME) results, and invokation of the Born and random-phase approximations generates a set of coupled Volterra-type integrodifferential equations (VTE)

$$\dot{P}_S(t) = \sum_{S' \neq S} \int_0^t dt' [K_{SS'}(t-t')P_{S'}(t') - K_{SS'}(t-t')\, P_S(t')] \quad , \tag{1}$$

where $P_S(t)$ is a diagonal matrix element of the projected density operator in the subspace $\mathcal{S}$, and represents the probability of finding $\mathcal{S}$ in an eigenstate $|S\rangle$ of the zero-order sub-Hamiltonian $\mathcal{H}_{\mathcal{S}}$:

$$\mathcal{H}_{\mathcal{S}}|S\rangle = \mathcal{E}_S|S\rangle \quad . \tag{2}$$

The kernel functions $K_{SS'}(t-t')$ include temporal correlations between dynamical variables of the reservoirs.[2] The resulting dependence of the state of $\mathcal{S}$ at any time t upon all previous times $t' \leq t$, the memory effect, is manifested in the convolution form of $K_{SS'}(t-t')$, the memory kernels.[3] For most real physical systems, the form of $K_{SS'}$ precludes an analytic closed-form solution, and often even step-by-step numerical integration.[4] When numerical solutions using alternative techniques such as the method of successive approximations[5] are possible, one is limited to small times. For example, for kernels with some form of periodicity, a fairly common situation, these times are of the order of

a few periods, which seldom correspond to macroscopic measurement times. The solutions are therefore of little use in suggesting or elucidating physical mechanisms.

The need for numerical solutions has, in the past, been circumvented by making the Markovian approximation (MA),[6,7] namely that the system is amnesic (has negligible memory). Thus the convolution-type kernels are assumed to be extremeley localized temporally,

$$K_{SS'}(t-t') = W_{SS'}\,\delta(t-t') \ , \tag{3}$$

which is tantamount to assuming that the probability functions are very slowly varying during the (small) period of time in which $K_{SS'}(t)$ changes substantially. This approximation is difficult to justify in general, and is in fact not justified if a locally correct solution is sought. This is because $P_S(t)$ must reflect the nature of $K_{SS'}(t)$ itself, and if the latter varies substantially in any time range, so must $P_S(t)$, at least locally in time. What makes the MA useful is its avowed ability to provide the rough behavior of $P_S(t)$ over long time periods. Thus on a coarse-grained time scale, the MA is expected to provide results roughly resembling the exact results.

Not all physical systems admit of the representation of $K_{SS'}(t-t')$ shown in Eq. (3), an important example being a system resonantly pumped by a continuous-wave laser and coupled to another reservoir.[7-9] For this important class of physical systems the kernels can, under favorable conditions to be described later, be written as sums of terms such as Eq. (3) and additional constants independent of time.[2] The resulting equations of motion are very different from those obtained using Eq. (3). The differences are quantified andhighlighted in this work, and it is shown that the results of the exactly-solvable equations with kernels including the constants provide an excellent

representation of the solutions. The MA, on the other hand, is shown to lead to probability profiles in gross disagreement with the exact results, especially for the short time scale.

The format of this paper is as follows. In Section II the basic theory is summarized, and the results of calculations are presented in Section III. Conclusions are given in Section IV.

II. The Isomnesic (Constant-Memory) Approximation

A system of great current interest that lends itself ideally as a vehicle for illustrating the various approximations for the memory kernel is an adatom adsorbed on a solid surface, vibrationally excited by an infrared continuous-wave laser, and coupled to phonon modes of the solid.[2,7-9] The system $\mathcal{S}$ is the adbond, viz, the bond resulting from the interaction of the adatom with the phonon-averaged motion of the lattice atoms;[10] the phonons and the laser are two independent, noninteracting reservoirs $\mathcal{R}_1$ and $\mathcal{R}_2$. Quantum theoretical treatments of this class of systems lead quite generally to a GME and a corresponding VTE, Eq. (1), with $P_S(t)$ representing the probability of finding the adbond in the eigenstate $|S\rangle$ of the zero-order adbond Hamiltonian $\mathcal{H}_S$. The kernels $K_{SS'}(t-t')$ incorporate the influence of the phonons and the laser.[2] We have partitioned the total Hamiltonian of the system in such a way that the perturbations which generate the kernels are traceless in their individual reservoir subspaces.[2,10] As a direct consequence, the total kernels separate into individual subspace kernels,

$$K_{SS'}(t) = K^{(p)}_{SS'}(t) + K^{(r)}_{SS'}(t), \tag{4}$$

where $K^{(p)}_{SS'}(t)$ is due to the phonon field alone and $K^{(r)}_{SS'}(t)$ is due to the laser radiation field alone. Using a one-dimensional model for the solid,

we have obtained the kernels in closed form and solved them numerically by an iterative technique[5] for times of the order of a few "periods" of $K_{SS'}(t)$. These periods are dictated by the characteristic frequencies of the phonons and the adbond (i.e., the Debye frequency ω_D and the transition frequencies $\omega_{SS'}$ for bound states of the Hamiltonian $\mathcal{H}_{ss}$), and the laser frequency ω_L all of which are $\sim 10^{12} - 10^{14}$ Hz (1-100 THz). The periods are therefore very small, being $\sim 10^{-12} - 10^{-14}$ s (1-.01 ps); consequently, the solutions of the VTE can be obtained numerically for times no larger than about 10 ps, which is certainly insufficient for the description of a physical or chemical process. In order to obtain solutions for longer times, an analytic solution must be sought.

We begin with the assertion that the physically important situation is one where the laser frequency and the Debye frequency equal different transition frequencies $\omega_{SS'}$ of the adbond.[2] For this case $K^{(r)}_{SS'}(t)$ becomes a constant $k_{SS'}$ (from the term with $|\omega_{SS'}| = \omega_L$) plus oscillating terms which we ignore in the sense of the rotating-wave approximation.[6] The phonon term, $K^{(p)}_{SS'}(t)$, has a complicated behavior typified by $K^{(p)}_{01}(t)$ in Fig. 1, but we note that it has appreciable magnitude for times $\sim$ 2 ps, and almost vanishes subsequently. If the mesh size of our theoretical experiment is no less than 2 ps, we can treat $K^{(p)}_{SS'}(t)$ as a delta function, so that, from Eq. (4),

$$K_{SS'}(t) = \Omega_{SS'}\,\delta(t) + k_{SS'}\,, \tag{5}$$

where

$$\Omega_{SS'} = \int_0^\infty dt\; K^{(p)}_{SS'}(t)\,. \tag{6}$$

In Eq. (5), the first term, originating from the coupling of the adbond to the phonons, is the amnesic or Markovian term, and would lead, in the absence of the laser term, to the elimination of all memory effects. The second term, due to

the resonant laser coupling, is the isomnesic non-Markovian term, and represents a constant memory effect all the way back to t=0.

The subsequent treatment is simplified by defining "diagonal" elements Ω_{SS} and k_{SS}, viz.

$$\Omega_{SS} = -\sum_{S' \neq S} \Omega_{SS'} , \tag{7}$$

$$k_{SS} = -\sum_{S' \neq S} k_{S'S} \tag{8}$$

and the notation

$$\underline{\Omega} \equiv \{\Omega_{SS'}\} , \tag{9a}$$

$$\underline{k} \equiv \{k_{SS'}\} , \tag{9b}$$

$$\underline{K}(t) \equiv \{K_{SS'}(t)\} , \tag{9c}$$

$$\underline{W} \equiv \{W_{SS'}\} , \tag{9d}$$

$$\underline{\Delta} \equiv \{\delta_{SS'}\} , \tag{9e}$$

$$\underline{P}(t) \equiv \{P_S(t)\} . \tag{9f}$$

The exact VTE may be written as

$$\dot{\underline{P}}(t) = \int_0^t dt' \, \underline{K}(t-t') \cdot \underline{P}(t') ; \tag{10}$$

in the isomnesic approximation (IA) it becomes

$$\dot{\underline{P}}(t) = \underline{k} \cdot \int_0^t dt' \, \underline{P}(t') + \underline{\Omega} \cdot \underline{P}(t) . \tag{11}$$

Formally this can be solved without any further approximations. Differentiating both sides of Eq. (11), we get the second-order differential equation

$$\ddot{\underline{P}}(t) = \underline{k} \cdot \underline{P}(t) + \underline{\Omega} \cdot \dot{\underline{P}}(t) , \tag{12}$$

whose Laplace transform,

$$\underline{M}(s)\cdot\underline{\mathcal{P}}(s) = \underline{T}(s) \ , \tag{13}$$

where

$$\underline{M}(s) \equiv \underline{k} + s\underline{\Omega} - s^2\underline{\Delta} \ , \tag{14}$$

$$\underline{T}(s) \equiv - s\underline{P}(0) \ , \tag{15}$$

and $\underline{\mathcal{P}}(s)$ is the Laplace transform of $\underline{P}(t)$, is easily inverted using the Heaviside expansion theorem.[11]

While this effectively eliminates the non-Markovian bottleneck without recourse to Eq. (3), it is instructive to generate solutions of a Markovian version of this class of problems. To do this, we have to make provisions for localizing $K^{(r)}_{SS'}$ in time. This brings to the fore the pervasive issue of time scales in dynamical many-body systems, our specific question being the relative degree of localization ascribable to $K^{(p)}_{SS'}$ and $K^{(r)}_{SS'}$. If the laser radiation is localized as a pulse, it can still extend over a period of time much longer than the extent of $K^{(p)}_{SS'}(t)$. In other words, the delta function representing $K^{(p)}_{SS'}(t)$ may be quite different from the delta function representing $K^{(r)}_{SS'}(t)$, and the former may in fact not really be considered as localized with respect to the latter. With these provisos in mind, we can proceed to write the Markovian version of Eqs. (5), (10), (12) and (13):

$$\underline{K}(t) = (\underline{\Omega} + \underline{f})\ \delta(t) \ , \tag{16}$$

$$\dot{\underline{P}}(t) = \underline{W} \cdot \underline{P}\ (t) \ , \tag{17}$$

$$\underline{J}(s) \cdot \underline{\mathcal{P}}(s) = \underline{U} \ , \tag{18}$$

where

$$\underline{f} = \underline{k}\ \tau \ , \tag{19}$$

$$\underline{W} = \underline{\Omega} + \underline{f} \ , \tag{20}$$

$$\underline{J}(s) = (\underline{\Omega} + \underline{f} - s\underline{\Delta}) \ , \tag{21}$$

$$\underline{U} = - \underline{P}(0) \ , \tag{22}$$

and τ represents the actual extent of the laser signal or a variable time parameter. Equation (17) is the well-known Pauli master equation (PME).[1,6]

To summarize the formulation, Eq. (10) is the exact GME with a convolution type kernel which makes solutions dificult for experimental times. If the kernel can be approximated as the sum of a very sharply peaked function due to the phonons plus a constant due to the laser (the isomnesic approximation), we get the simplified GME, Eq. (11), which is still not Markovian but has a "constant memory" (isomnesic-) term. The resulting second-order differential equation, Eq. (12), can be solved analytically for arbitrarily long times. If, on the other hand, memory effects are assumed to be negligible, i.e., with a kernel highly localized in time, Eq. (3), we get the Markovian limit, namely the PME, Eq. (17), which is a first-order differential equation and can also be solved analytically for arbitrarily long times. The nature of the solutions depends, of course, on the time paramter τ in Eq. (19).

III. Results of the Exact, Isomnesic and Markovian Approximations

For a linear-chain model of the solid, the exact kernel function due to phonons alone, $\underline{K}^{(p)}$, involves an expansion over the number of phonons n and the number of lattice atoms ℓ. For the specific system chosen, the effective surface potential generates five bound states; we have chosen $|\omega_{01}| = \omega_D$ and $|\omega_{13}| = \omega_L$ [$\omega_{SS'} = (\mathcal{E}_S - \mathcal{E}_{S'})/\hbar$; see Eq. (2)]. The phonon kernels, e.g., $K_{01}^{(p)}(t)$ in Fig. 1, fall off quite rapidly in time and arise almost entirely from the ($n=1$, $\ell=1$) term.

At issue is the validity of the isomnesic and Markovian approximations. We can examine two aspects of the results, viz. the details of the early transient behavior, and the long-term steady state. For the Markovian case, we can further examine the effects of varying τ in Eq. (19). The transient behavior can be compared with exact numerical solutions of Eq. (10), but the steady-state results of the MA and the IA can only be judged by extrapolation.

While the probability profiles $\underline{P}(t)$ provide sufficient comparison, the physical contents of our results are better displayed by the average adbond energy given by

$$\mathcal{E}(t) = \sum_S P_S(t)\mathcal{E}_S \ , \tag{23}$$

where $\mathcal{E}_S$ is the energy eigenvalue corresponding to the level $|S\rangle$ of the effective adbond potential. This provides a simple measure of the chemical direction of the adbond and a *well-defined connection between this exact theory* and phenomenological models of such processes.

The results obtained by solving Eqs. (10), (12) and (17) for a variety of situations of physical interest are very consistent, and we present a typical set of curves in Fig. 2 for early times, $t \leq 5$ ps. The exact results are rich in detail and, to a large degree, follow the variations in $\underline{\underline{K}}(t)$. We shall not dwell on the physical contents except to mention the conspicuous absence of the simple exponential approach to equilibrium postulated in relaxation time theories. The results of the IA, while exhibiting the expected loss of the fine detail, are seen to chart out the <u>average</u> behavior of $\underline{P}(t)$ with great accuracy. Thus, for example, the crossing point of $P_1(t)$ and $P_3(t)$ is reproduced at $t = 1.7$ ps as compared to the exact crossing point at 2.2 ps, and the difference $P_1(t) - P_3(t)$ is seen to follow the exact difference with a similar slight

temporal retardation. The gross oscillations of $\underline{P}(t)$ are also reproduced faithfully. Consequently, we feel confident in our prediction that the steady-state results of the IA will conform to the exact results very accurately. We wish to emphasize the significance of this. The IA makes possible the complete solution of a GME for arbitrarily long times, when the solution of the exact GME is essentially impossible. The solution of the GME in the IA is no more difficult than that of the PME obtained by invoking the MA which, however, gives results which differ radically from the exact results in the transient region for a wide range of values of τ. Figure 3 illustrates the variations of $P_S(t)$ with τ in the MA (10^{-5} ps $\leq \tau \leq 10^{5}$ ps). The probability profiles are seen to be insensitive to increases in τ beyond ~ 10 ps, which corresponds to almost instantaneous saturation. The apparent insensitivity of $\underline{P}(t)$ for $\tau \leq 10^{-2}$ ps seen in Fig. 3 is, of course, misleading, since in this region the $P_S(t)$ vary with time too slowly for the change to be evident in the 20 ps time range of the plot. Drawn for 2 ns in Fig. 4 [we present only $P_3(t)$], the differences become more pronounced for $\tau \leq 10^{-2}$ ps, and the strong dependence of the apparent "equilibration time" on τ emerges clearly. We see no unambiguous way of choosing an appropriate value for τ. For systems which are known or expected to equilibrate very quickly, one could make an ad hoc semiempirical choice of τ to solve a PME for the steady state. However, if one is interested in the details of the short-time behavior of the system, one must solve the GME using the IA.

For comparison of the MA with the IA we have chosen $\tau = 1$ ps. The resulting profiles for the MA are shown in Fig. 5, along with our IA results for 20 ps. The complete absence of oscillatory behavior representing beats of the system and of population crossings, and the presence of predominantly exponential variation of $\underline{P}(t)$ representative of a "relaxation time" exhibited by the MA

results of Fig. 5 are not necessarily general features of the solutions of a PME. Since the matrices $\underline{M}$ and $\underline{J}$ are, in general, asymmetric, both the GME and the PME can generate oscillatory solutions $\underline{P}(t)$, contradicting earlier contentions.[12] However, the total lack of resemblance between the early PME results and the exact ones for the present case is alarming and raises urgent and serious questions about the validity of the Markovian approximation, even for a rough qualitatiave estimate of the early transient behavior of many-body systems with a nonrandom force. At best, these results suggest the need for great caution in using the MA. In retrospect this is not surprising, because the representation of a time-independent cw laser beam by an ultrashort pulse is tenuous, whereas that of the very-short-range (in time) phonon correlation by a delta function is quite reasonable.

The results for $\mathcal{E}(t)$, shown in Fig. 6 for the exact GME and the IA and in Fig. 7 for the MA and the IA further support these contentions. The IA generates an energy profile which, except for a slight temporal retardation, is a low-resolution representation of the exact result. The significant increase in the bond energy at the expense of both the laser and the solid is clearly evident in the IA results of Figs. 2 and 6. The results of the MA are qualitatively different from the exact and IA results, and describe a monotonic approach to the steady state. The exact and IA results show actual periodic energy transfer out of the adbond followed by successive build up due to overall energy inflow. The apparent correspondence seen in Fig. 7 between the magnitude of $\mathcal{E}(t)$ in the MA and the "base line" about which the results of the exact GME and the IA oscillate is entirely due to our choice of $\tau = 1$ ps. That no such correspondence can be expected in general is evident from Fig. 8 showing the variations of $\mathcal{E}(t)$ with τ. The steady-state ($t \to \infty$) values of $\underline{P}(t)$ and $\mathcal{E}(t)$ in

the MA have been found to be the same as those obtained with the IA for all cases considered so far (when the values of τ chosen lead to steady states in the time ranges considered).

IV. Conclusion

Our results for the time evolution of a dynamical many-body system subject to a variety of forces point out the inadequacies of the Markovian approximation when the resulting memory kernel is nonlocal in time. As an alternative, we present the isomnesic approximation which is characterized by a constant memory; this eliminates the non-Markovian bottleneck associated with the convolution-type memory kernel in the Volterra-type integrodifferential equation resulting from the generalized master equation. Closed solutions of the latter are in excellent agreement with the exact results, in contrast to those of the Markovian approximation.

Acknowledgements

This research was supported by the Office of Naval Research, the Air Force Office of Scientific Research (AFSC), United States Air Force under Grant AFOSR-82-0046, and the National Science Foundation under Grant CHE-8320185. The United States Government is authorized to reproduce and distribute reprints for governmental purposes notwithstanding any copyright notation hereon. TFG acknowledges the Camille and Henry Dreyfus Foundation for a Teacher-Scholar Award (1975-86).

References

1. F. Haake, in Springer Tracts in Modern Physics, edited by G. Höhler (Springer-Verlag, Berlin, 1973), p. 98ff.

2. A. C. Beri and Thomas F. George, unpublished.

3. R. W. Zwanzig, in Lectures in Theoretical Physics, Vol. III, edited by W. E. Brittin, B. W. Downs and J. Downs (Interscience Publishers, New York, 1961), p. 106ff.

4. See, for example, Treatment of Integral Equations by Numerical Methods edited by C. T. H. Baker and G. F. Miller (Academic Press, New York, 1982) and Numerical Treatment of Integral Equations edited by J. Albrecht, Clausthal-Zellerfeld and L. Collatz (Birkhäuser Verlag, Basel, 1980).

5. L. Collatz, "The Numerical Treatment of Differential Equations" (Springer-Verlag, New York, 1966), Chapter VI.

6. W. H. Louisell, "Quantum Statistical Properties of Radiation" (John Wiley & Sons, New York, 1973), Chapter 6.

7. J. Lin, A. C. Beri, M. Hutchinson, W. C. Murphy and T. F. George, Phys. Lett. 79A, 233 (1980).

8. T. F. George, A. C. Beri, K. S. Lam and J. Lin, in Laser Applications, edited by J. F. Ready and R. K. Erf (Academic Press, New York, 1984), pp. 69-127; T. F. George, J. Lin, A. C. Beri and W. C. Murphy, Prog. Surf. Sci., in press.

9. C. Jedrzejek, K. F. Freed, S. Efrima and H. Metiu, Surf. Sci. 109, 191 (1981).

10. C. Jedrzejek, K. F. Freed, E. Hood and H. Metiu, J. Chem. Phys. 79, 2436 (1983).

11. E. Butkov, "Mathematical Physics", (Addison Wesley Publishing Co., Reading, Massachusetts, 1968), Chapter 5.

12. A. Janner, L. Van Hove and E. Verboven, Physica 28, 1341 (1962).

Figure Captions

Fig. 1. The phonon part $K_{01}^{(P)}(t)$ of the memory kernel.

Fig. 2. Probability profiles $P_S(t)$ for levels S= 0, 1 and 3 of the adbond. Solid lines: Exact numerical solutions of the GME; broken lines: closed-form solutions of the GME with the IA.

Fig. 3. $P_S(t)$ for the system of Fig. 2 with the MA for a ten-decade range of τ. (A)-$P_0(t)$; (B)-$P_1(t)$; (C)-$P_3(t)$.

Fig. 4. $P_3(t)$ with the MA for 2 ns.

Fig. 5. Comparison of $P_S(t)$ with the IA (solid lines) and the MA (τ=1 ps; broken lines) for S=0, 1 and 3

Fig. 6. Average adbond energy $\mathcal{E}(t)$ obtained via the numerical solution of the exact GME (solid line) and closed-form solution with the IA (broken line).

Fig. 7. $\mathcal{E}(t)$ with the IA (solid line) and the MA (τ=1 ps; broken line).

Fig. 8. Variation of $\mathcal{E}(t)$ with τ in the MA.

MEMORY KERNEL

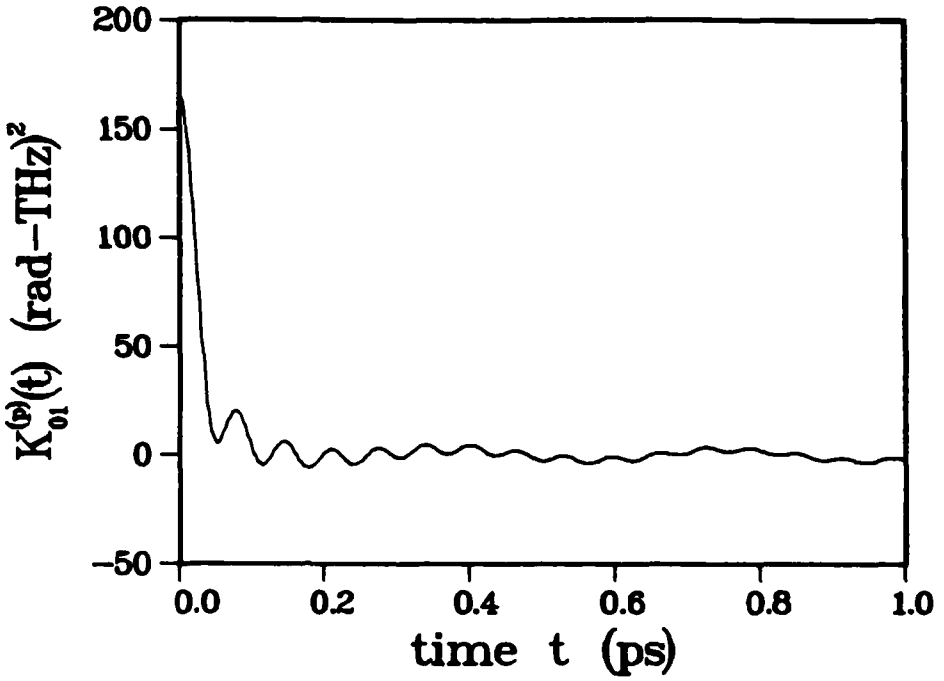

Ben/George Fig 1

EXACT vs. *ISOMNESIC*

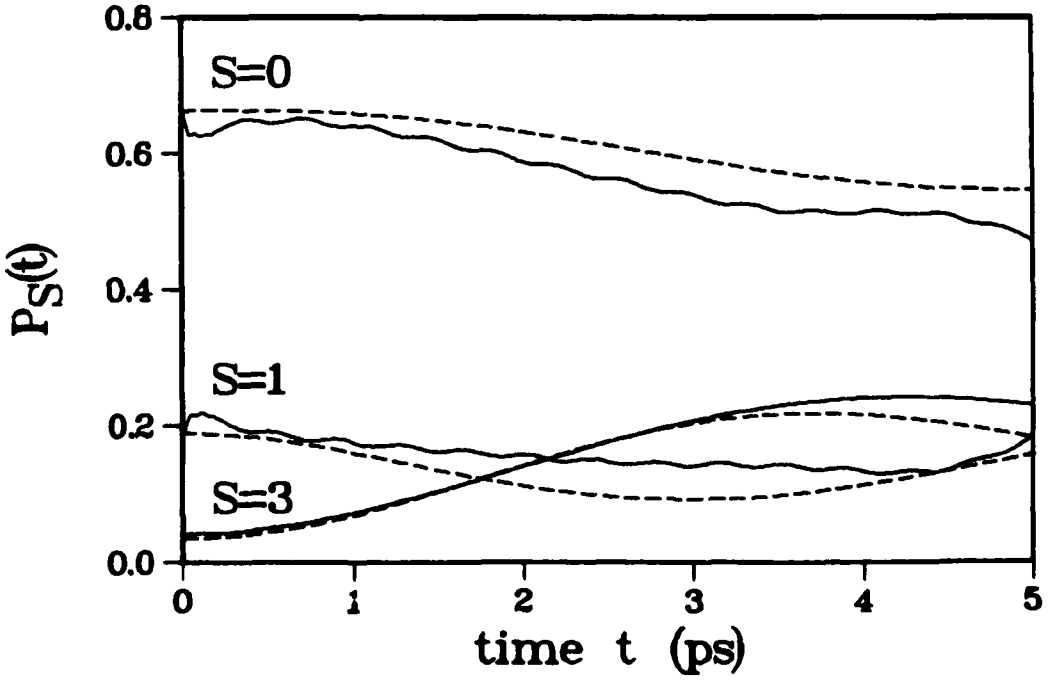

Ben/George Fig 2

MARKOVIAN APPROXIMATION

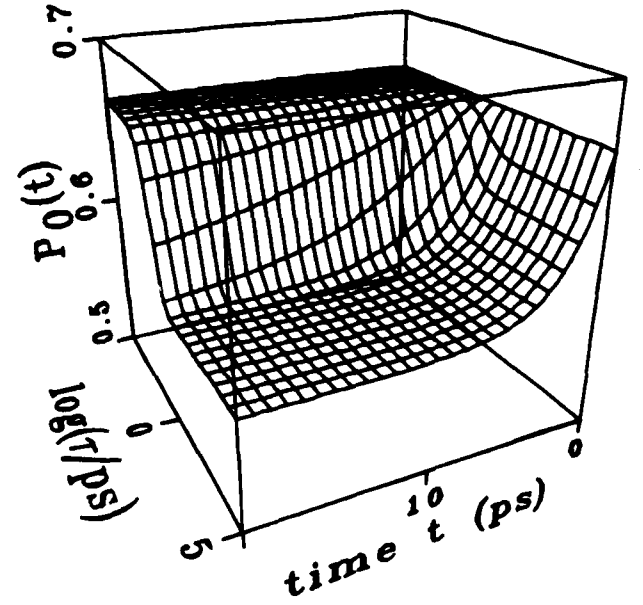

(A)

Beri/George Fig 3(A)

MARKOVIAN APPROXIMATION

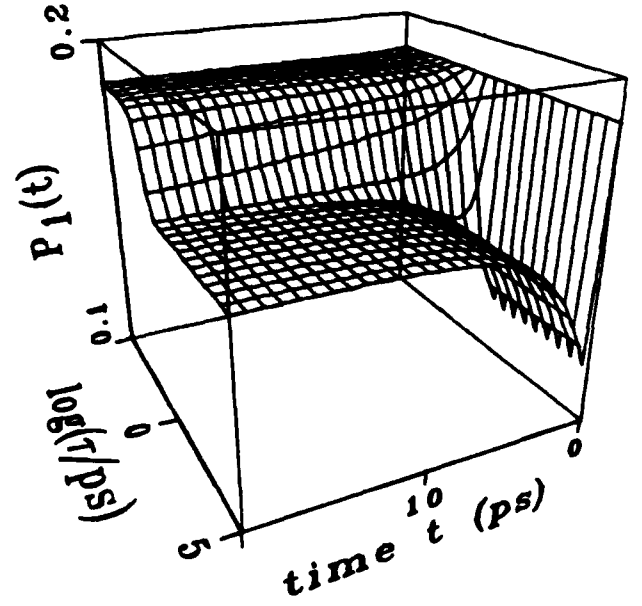

(B)

Beri/George Fig 3(B)

MARKOVIAN APPROXIMATION

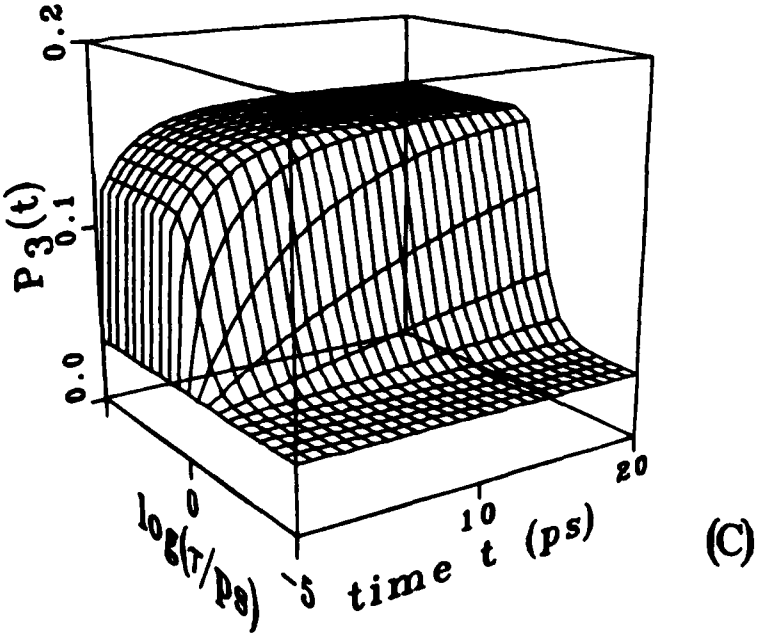

(C)

Beri/George Fig 3(c)

MARKOVIAN APPROXIMATION

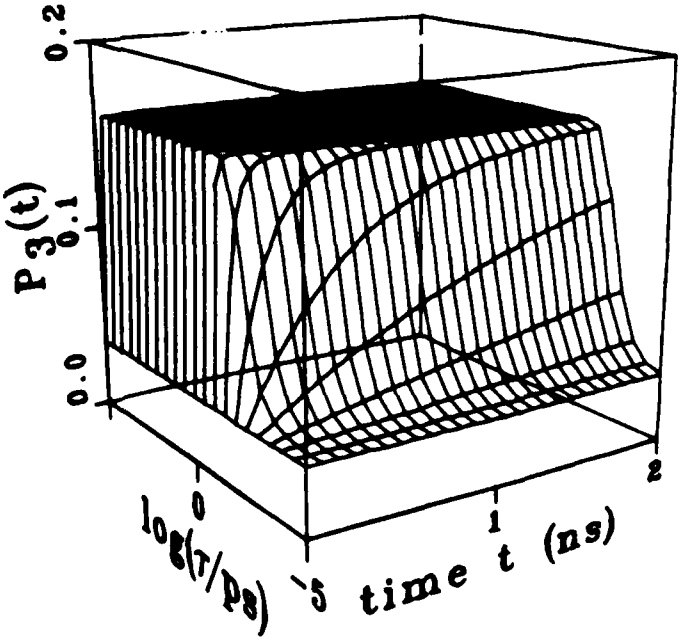

Beri/George Fig 4

ISOMNESIC vs. *MARKOVIAN*

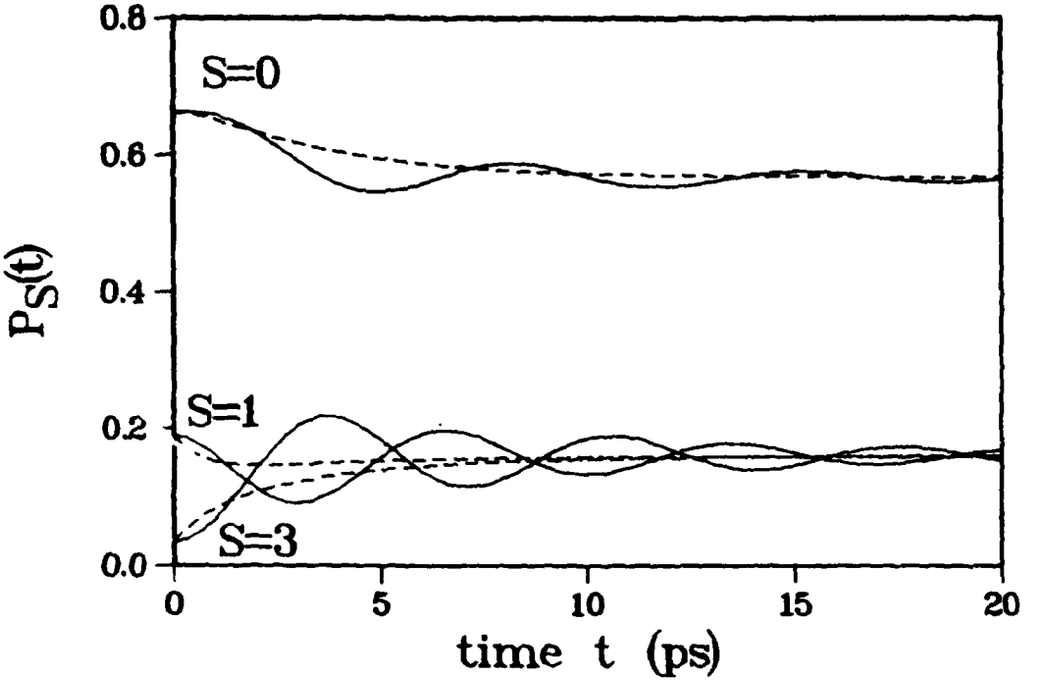

Beri/George Fig 5

EXACT vs. *ISOMNESIC*

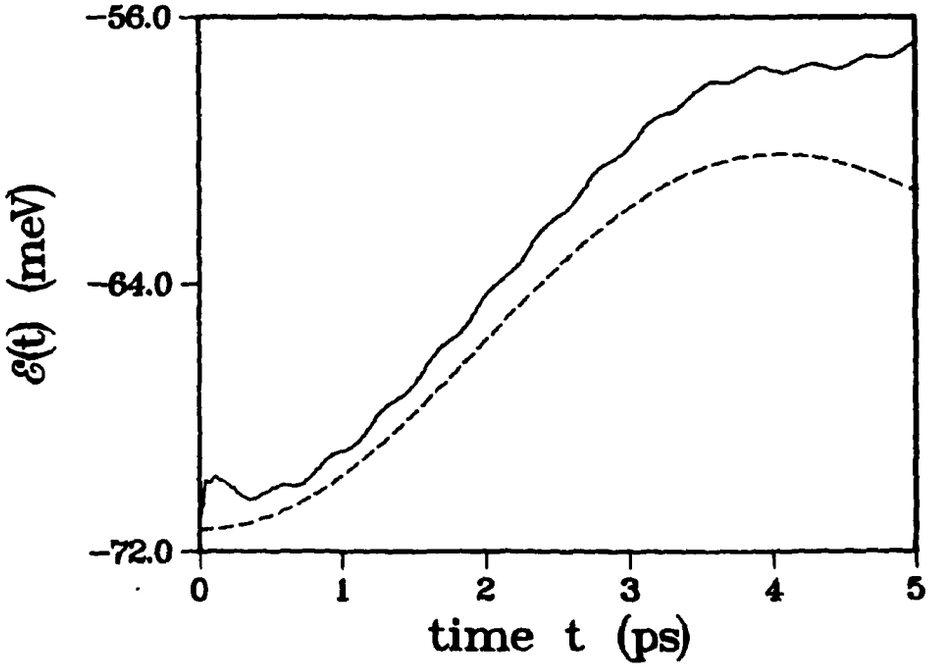

Beri/George Fig 6

ISOMNESIC vs. *MARKOVIAN*

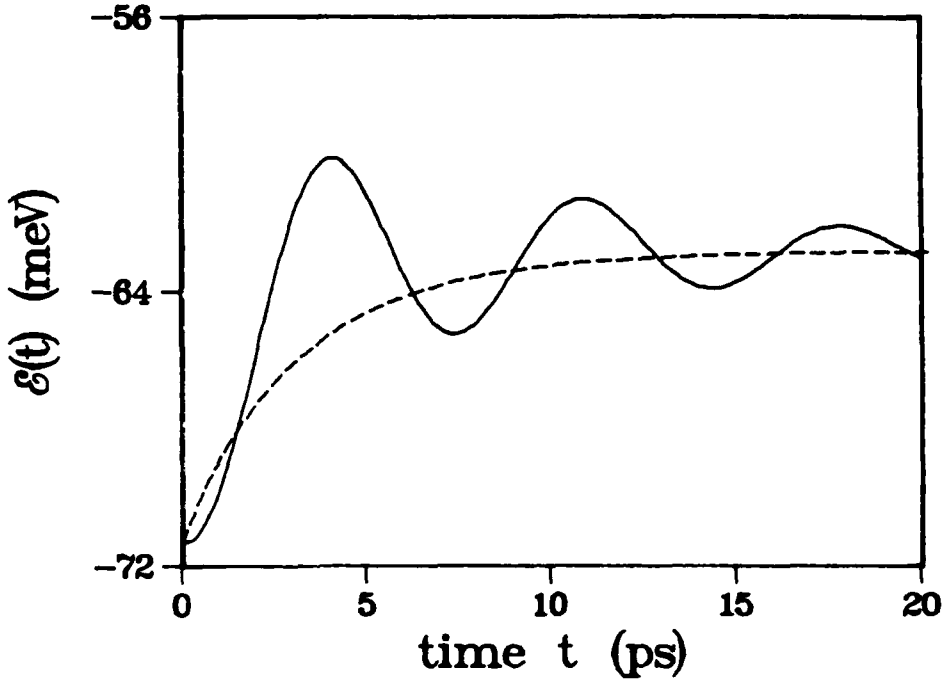

Ber/George Fig 7

MARKOVIAN APPROXIMATION

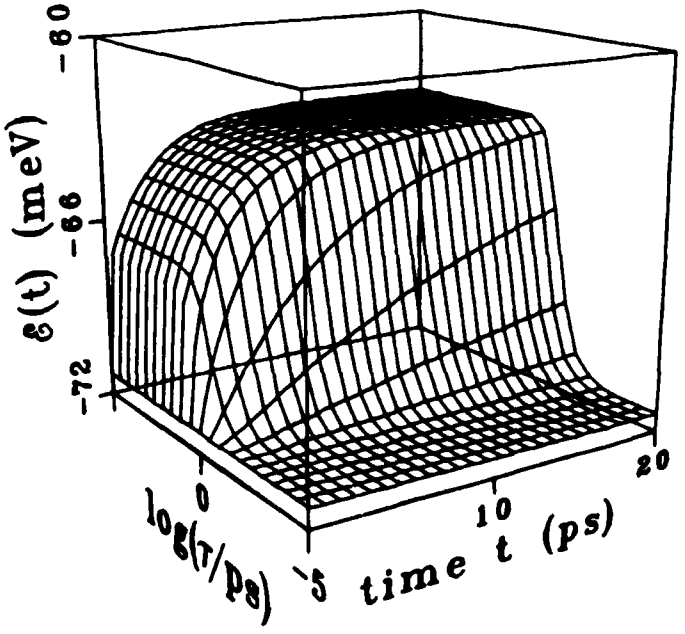

Ber/George Fig

DL/413/83/01
GEN/413-2

TECHNICAL REPORT DISTRIBUTION LIST, GEN

	No. Copies
Office of Naval Research Attn: Code 413 800 N. Quincy Street Arlington, Virginia 22217	2
Dr. Bernard Douda Naval Weapons Support Center Code 5042 Crane, Indiana 47522	1
Commander, Naval Air Systems Command Attn: Code 310C (H. Rosenwasser) Washington, D.C. 20360	1
Naval Civil Engineering Laboratory Attn: Dr. R. W. Drisko Port Hueneme, California 93401	1
Defense Technical Information Center Building 5, Cameron Station Alexandria, Virginia 22314	12
DTNSRDC Attn: Dr. G. Bosmajian Applied Chemistry Division Annapolis, Maryland 21401	1
Dr. William Tolles Superintendent Chemistry Division, Code 6100 Naval Research Laboratory Washington, D.C. 20375	1
Dr. David Young Code 334 NORDA NSTL, Mississippi 39529	1
Naval Weapons Center Attn: Dr. A. B. Amster Chemistry Division China Lake, California 93555	1
Scientific Advisor Commandant of the Marine Corps Code RD-1 Washington, D.C. 20380	1
U.S. Army Research Office Attn: CRD-AA-IP P.O. Box 12211 Research Triangle Park, NC 27709	1
Mr. John Boyle Materials Branch Naval Ship Engineering Center Philadelphia, Pennsylvania 19112	1
Naval Ocean Systems Center Attn: Dr. S. Yamamoto Marine Sciences Division San Diego, California 91232	1
Dr. David L. Nelson Chemistry Division Office of Naval Research 800 North Quincy Street Arlington, Virginia 22217	1

DL/413/83/01
056/413-2

ABSTRACTS DISTRIBUTION LIST, 056/625/629

Dr. G. A. Somorjai
Department of Chemistry
University of California
Berkeley, California 94720

Dr. J. Murday
Naval Research Laboratory
Surface Chemistry Division (6170)
455 Overlook Avenue, S.W.
Washington, D.C. 20375

Dr. J. B. Hudson
Materials Division
Rensselaer Polytechnic Institute
Troy, New York 12181

Dr. Theodore E. Madey
Surface Chemistry Section
Department of Commerce
National Bureau of Standards
Washington, D.C. 20234

Dr. J. E. Demuth
IBM Corporation
Thomas J. Watson Research Center
P.O. Box 218
Yorktown Heights, New York 10598

Dr. M. G. Lagally
Department of Metallurgical
and Mining Engineering
University of Wisconsin
Madison, Wisconsin 53706

Dr. R. P. Van Duyne
Chemistry Department
Northwestern University
Evanston, Illinois 60637

Dr. J. M. White
Department of Chemistry
University of Texas
Austin, Texas 78712

Dr. D. E. Harrison
Department of Physics
Naval Postgraduate School
Monterey, California 93940

Dr. W. Kohn
Department of Physics
University of California, San Diego
La Jolla, California 92037

Dr. R. L. Park
Director, Center of Materials
Research
University of Maryland
College Park, Maryland 20742

Dr. W. T. Peria
Electrical Engineering Department
University of Minnesota
Minneapolis, Minnesota 55455

Dr. Keith H. Johnson
Department of Metallurgy and
Materials Science
Massachusetts Institute of Technology
Cambridge, Massachusetts 02139

Dr. S. Sibener
Department of Chemistry
James Franck Institute
5640 Ellis Avenue
Chicago, Illinois 60637

Dr. Arold Green
Quantum Surface Dynamics Branch
Code 3817
Naval Weapons Center
China Lake, California 93555

Dr. A. Wold
Department of Chemistry
Brown University
Providence, Rhode Island 02912

Dr. S. L. Bernasek
Department of Chemistry
Princeton University
Princeton, New Jersey 08544

Dr. P. Lund
Department of Chemistry
Howard University
Washington, D.C. 20059

DL/413/83/01
056/413-2

ABSTRACTS DISTRIBUTION LIST, 056/625/629

Dr. F. Carter
Code 6132
Naval Research Laboratory
Washington, D.C. 20375

Dr. Richard Colton
Code 6112
Naval Research Laboratory
Washington, D.C. 20375

Dr. Dan Pierce
National Bureau of Standards
Optical Physics Division
Washington, D.C. 20234

Dr. R. Stanley Williams
Department of Chemistry
University of California
Los Angeles, California 90024

Dr. R. P. Messmer
Materials Characterization Lab.
General Electric Company
Schenectady, New York 22217

Dr. Robert Gomer
Department of Chemistry
James Franck Institute
5640 Ellis Avenue
Chicago, Illinois 60637

Dr. Ronald Lee
R301
Naval Surface Weapons Center
White Oak
Silver Spring, Maryland 20910

Dr. Paul Schoen
Code 5570
Naval Research Laboratory
Washington, D.C. 20375

Dr. John T. Yates
Department of Chemistry
University of Pittsburgh
Pittsburgh, Pennsylvania 15260

Dr. Richard Greene
Code 5230
Naval Research Laboratory
Washington, D.C. 20375

Dr. L. Kesmodel
Department of Physics
Indiana University
Bloomington, Indiana 47403

Dr. K. C. Janda
California Institute of Technology
Division of Chemistry and Chemical Engineering
Pasadena, California 91125

Dr. E. A. Irene
Department of Chemistry
University of North Carolina
Chapel Hill, Northc Carolina 27514

Dr. Adam Heller
Bell Laboratories
Murray Hill, New Jersey 07974

Dr. Martin Fleischmann
Department of Chemistry
Southampton University
Southampton 509 5NH
Hampshire, England

Dr. John W. Wilkins
Cornell University
Laboratory of Atomic and Solid State Physics
Ithaca, New York 14853

Dr. Richard Smardzewski
Code 6130
Naval Research Laboratory
Washington, D.C. 20375

Dr. H. Tachikawa
Chemistry Department
Jackson State University
Jackson, Mississippi 39217

DL/413/83/01
056/413-2

ABSTRACTS DISTRIBUTION LIST, 056/625/629

Dr. R. G. Wallis
Department of Physics
University of California
Irvine, California 92664

Dr. D. Ramaker
Chemistry Department
George Washington University
Washington, D.C. 20052

Dr. J. C. Hemminger
Chemistry Department
University of California
Irvine, California 92717

Dr. T. F. George
Chemistry Department
University of Rochester
Rochester, New York 14627

Dr. G. Rubloff
IBM
Thomas J. Watson Research Center
P.O. Box 218
Yorktown Heights, New York 10598

Dr. Horia Metiu
Chemistry Department
University of California
Santa Barbara, California 93106

Captain Lee Myers
AFOSR/NC
Bollig AFB
Washington, D.C. 20332

Dr. J. T. Keiser
Department of Chemistry
University of Richmond
Richmond, Virginia 23173

Dr. Roald Hoffmann
Department of Chemistry
Cornell University
Ithaca, New York 14853

Dr. R. W. Plummer
Department of Physics
University of Pennsylvania
Philadelphia, Pennsylvania 19104

Dr. E. Yeager
Department of Chemistry
Case Western Reserve University
Cleveland, Ohio 41106

Dr. N. Winograd
Department of Chemistry
Pennsylvania State University
University Park, Pennsylvania 16802

Dr. G. D. Stein
Mechanical Engineering Department
Northwestern University
Evanston, Illinois 60201

Dr. A. Steckl
Department of Electrical and
Systems Engineering
Rensselaer Polytechnic Institute
Troy, NewYork 12181

Dr. G. H. Morrison
Department of Chemistry
Cornell University
Ithaca, New York 14853

Dr. P. Hansma
Physics Department
University of California
Santa Barbara, California 93106

Dr. J. Baldeschwieler
California Institute of Technology
Division of Chemistry
Pasadena, California 91125

Dr. W. Goddard
California Institute of Technology
Division of Chemistry
Pasadena, California 91125

DL/413/83/01
056/413-2

ABSTRACTS DISTRIBUTION LIST, 056/625/629

Dr. J. E. Jensen
Hughes Research Laboratory
3011 Malibu Canyon Road
Malibu, California 90265

Dr. W. Knauer
Hughes Research Laboratory
3011 Malibu Canyon Road
Malibu, California 90265

Dr. J. H. Weaver
Department of Chemical Engineering
and Materials Science
University of Minnesota
Minneapolis, Minnesota 55455

Dr. C. B. Harris
Department of Chemistry
University of California
Berkeley, California 94720

END

FILMED

7-85

DTIC